Supplementary Material

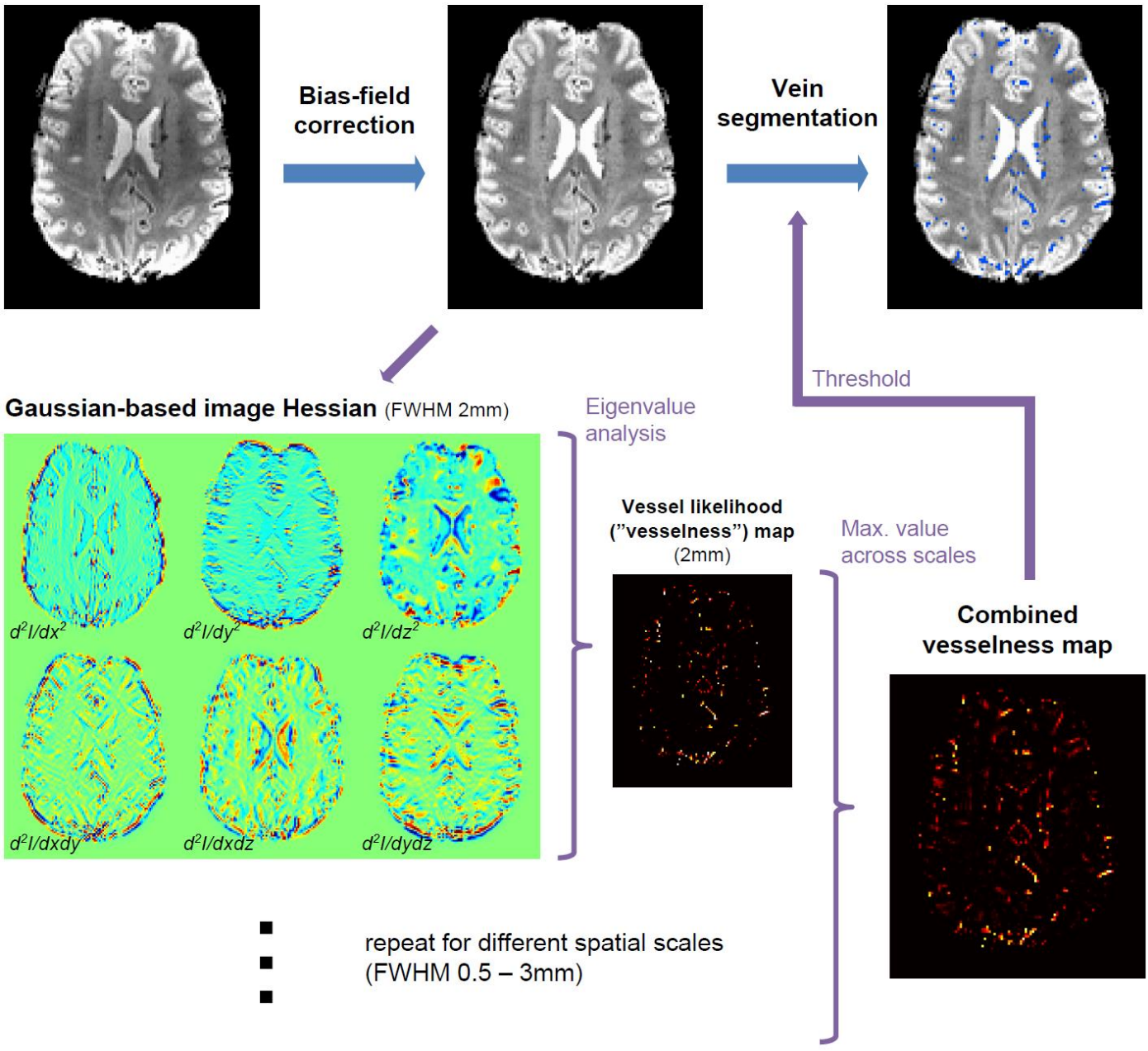

Supp. Fig. 1. Schematic representation of the vein segmentation procedure adopted in this work. For each EPI dataset, the (unsmoothed) volume used as reference for motion correction was first bias field-corrected (using FSL-FAST), and then analyzed with multiscale vessel enhancement filtering (Frangi et al., 1998). This technique explores the local second-order structure (curvature) information in the image, based on the eigenvalues of the local 3D Gaussian-based Hessian matrix. Different spatial scales (vessel thicknesses) can be probed by adjusting the Gaussian FWHM, and finally combined to yield a multiscale vessel likelihood map. This map can then be thresholded to obtain a vein mask.

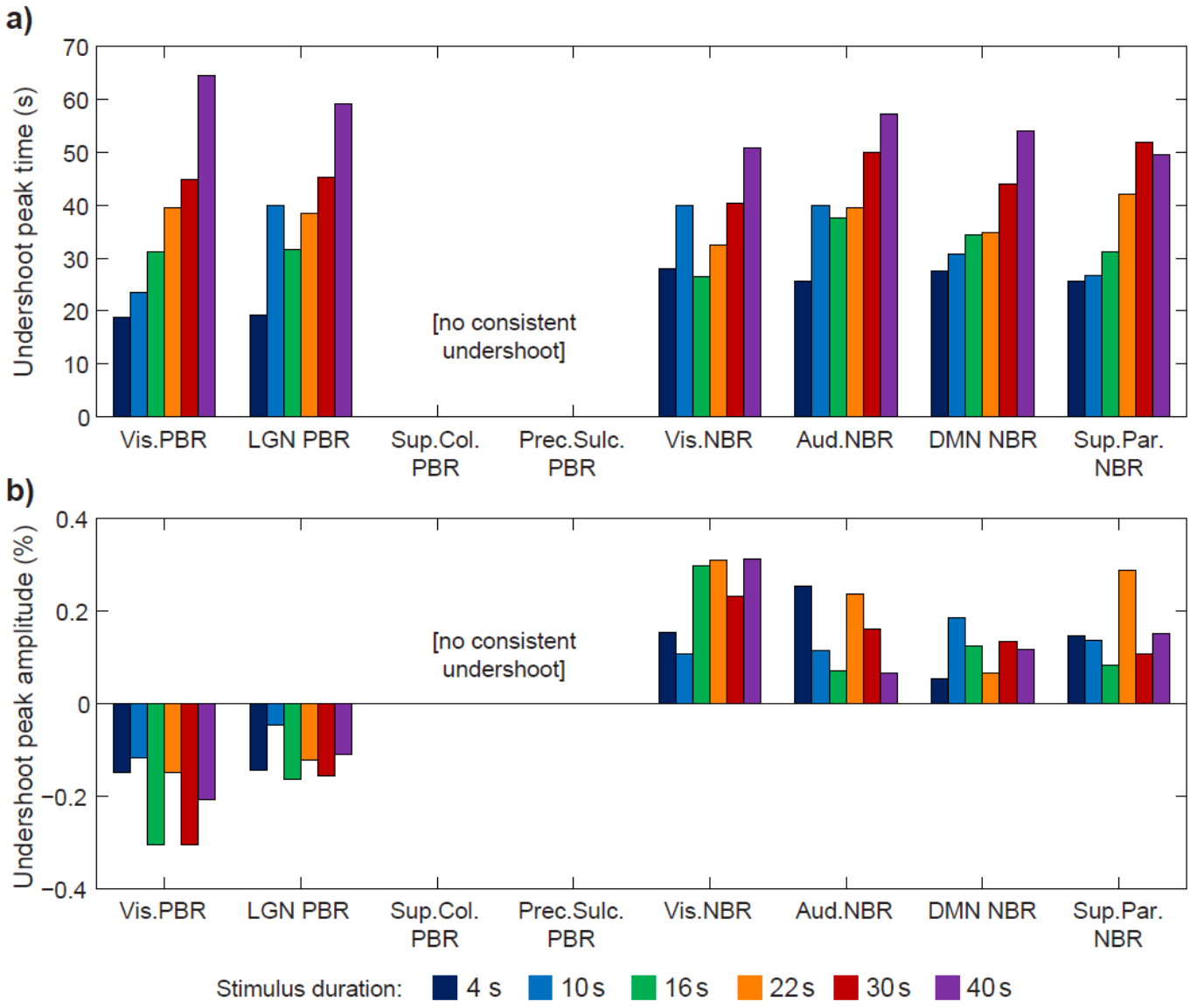

Supp. Fig. 2. Properties of group average BOLD response under/overshoots as a function of stimulus duration (*FDur*), in multiple brain regions. The estimation of (a) time to peak and (b) peak amplitude were performed directly on the group-averaged BOLD responses (Fig. 2).

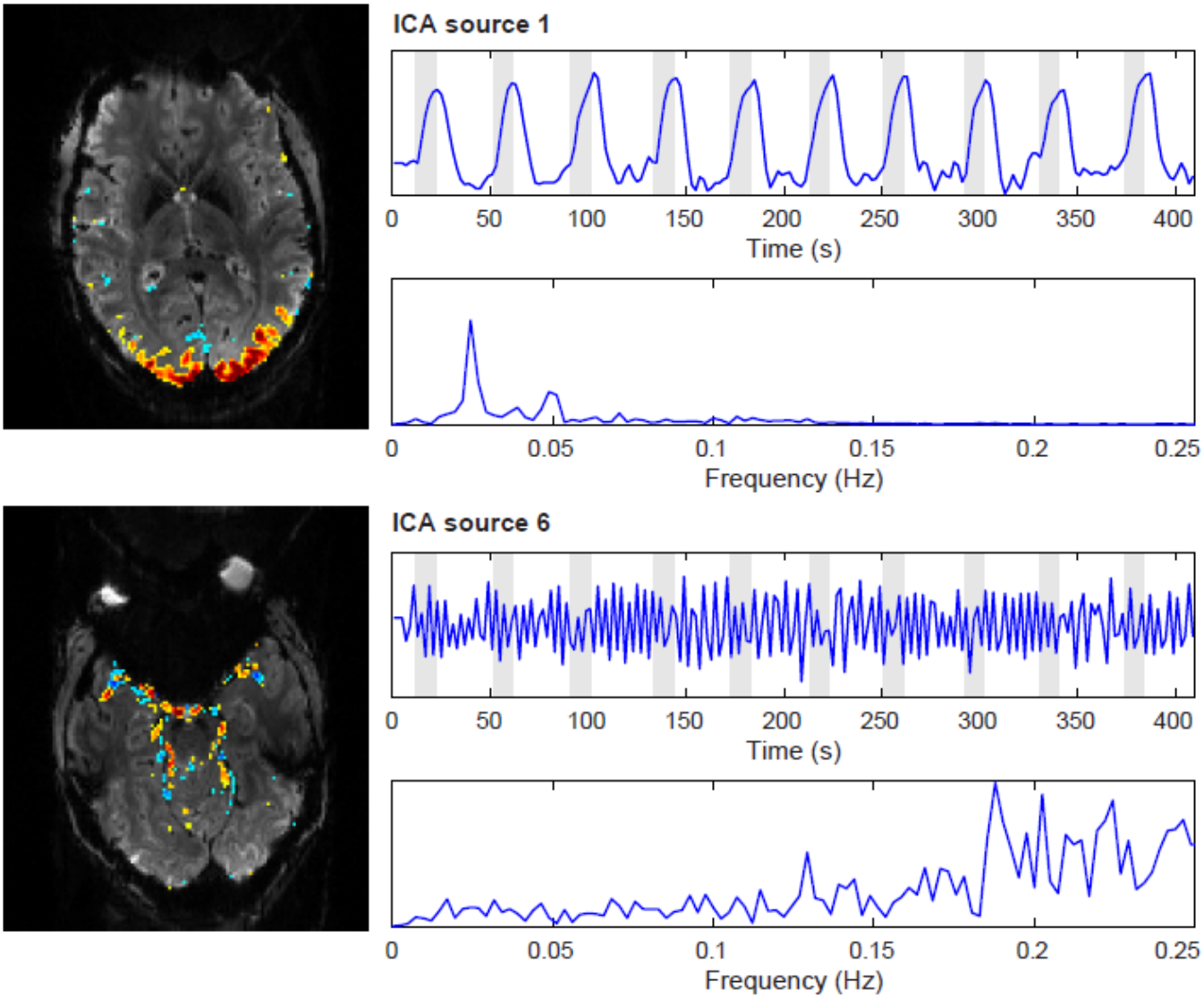

Supp. Fig. 3. Maps, timecourses and spectra of typical independent components obtained from ICA decomposition in an example subject. The examples shown correspond to a paradigm-related (top) and physiological noise source, likely of cardiac origin (bottom). These components were systematically encountered across subjects. Component maps (left) have been thresholded and overlaid on the reference EPI volume for visualization.

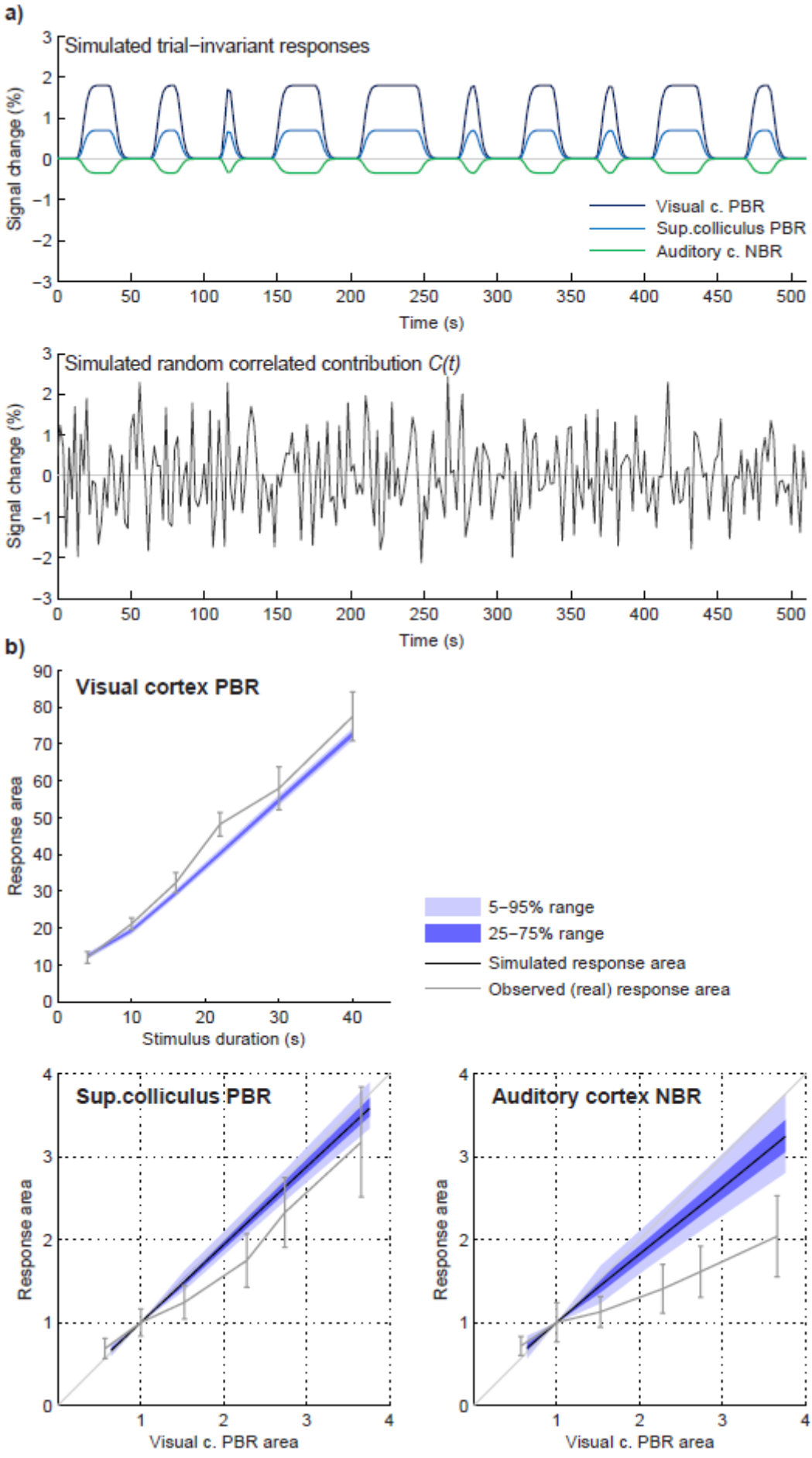
a)
Simulated trial−invariant responses
Signal change (%)
Time (s)
Visual c. PBR
Sup.colliculus PBR
Auditory c. NBR
Simulated random correlated contribution C(t)
Signal change (%)
Time (s)
b)
Visual cortex PBR
Response area
Stimulus duration (s)
5−95% range
25−75% range
Simulated response area
Observed (real) response area
Sup.colliculus PBR
Response area
Visual c. PBR area
Auditory cortex NBR
Response area
Visual c. PBR area

Supp. Fig. 4. Numerical simulations performed to evaluate the impact of signal contributions that vary across trials but are positively correlated between PBR and NBR regions, as reported by Mayhew et al. (2016), on the deviations between PBR and NBR areas observed in this work. Mayhew et al. (2016) attributed a substantial part of these fluctuations to contributions from the global brain signal and related to vascular reactivity, but another part remained unaccounted for, and deemed to possibly originate from real fluctuations in local neuronal activity. For the numerical simulations, three regions were considered: visual cortex (PBR), sup. colliculus (PBR) and auditory cortex (NBR) – these regions exhibited the strongest PBR and the weakest PBR and NBR, respectively. BOLD responses to the *FDur* paradigm were simulated for these regions with a sum of the six paradigm regressors, thereby assuming the same dependence on stimulus duration for all regions; response amplitudes were scaled according to the real response peaks observed for 10s-stimuli (1.8%, 0.70% and -0.35% signal change, respectively for each region (Fig. 2)). A fluctuation timecourse *C(t)* was created with random spectral distribution, to represent any potential combination of random/unknown contributions; slow drift was modeled and regressed out of *C(t)* (as would happen in the real GLM analyses), and its root-mean-square was scaled to match the variability found in real responses, after GLM analysis – approximately 0.42% signal change (Fig. 7b, green bars). *C(t)* was then added equally to each of the region responses. This process was performed 10 times to simulate a subject group (different *C(t)* for each subject), and average response areas were estimated exactly as in the real case (Fig. 3). The subject group was simulated 1000 times, all with different *C(t)* timecourses. b) Distribution of simulated outcomes for the relationship between the visual cortex PBR area and stimulus duration, and between the response areas of the three regions. The blue-colored margins delimitate the distribution of 5-95% (light blue) and 25-75% (dark blue) of the simulation outcomes. The black line depicts the median outcome, and the grey error bars depict the real observed outcome for the same regions (the same as in Fig. 3). Additionally to these results, further tests were performed where *C(t)* was given a random spectral distribution only in the 0.01–0.1 Hz frequency range and zero power elsewhere, to simulate a scenario where the random contribution is dominated by resting-state fluctuations (neuronal or non-neuronal in origin). In this case, the small deviation between the visual cortex PBR and auditory cortex NBR areas became slightly more accentuated, and the margin of simulated outcomes was slightly widened; nevertheless, the real NBR deviations observed in the data (grey error bars) remained outside the range of simulated outcomes.